We are IntechOpen, the world's leading publisher of Open Access books
Built by scientists, for scientists

6,900
Open access books available

185,000
International authors and editors

200M
Downloads

154
Countries delivered to

Our authors are among the

TOP 1%
most cited scientists

12.2%
Contributors from top 500 universities

CLARIVATE ANALYTICS
BOOK CITATION INDEX
INDEXED

WEB OF SCIENCE™

Selection of our books indexed in the Book Citation Index
in Web of Science™ Core Collection (BKCI)

Interested in publishing with us?
Contact book.department@intechopen.com

Numbers displayed above are based on latest data collected.
For more information visit www.intechopen.com

Designing Nanocrystal Electrodes by Supercritical Fluid Process and Their Electrochemical Properties

Dinesh Rangappa and Itaru Honma
Institute of Multidisciplinary Research for Advanced Materials, Tohoku University
2-1-1, Katahira, Aoba-ku, Sendai 980-8577
Japan

1. Introduction

Modern society's dependence on the electrical appliances and portable electronics has made rigorours development in battery technology. After three decades of development in battery technology, the Li-ion battery technology has emerged as one of the most popular battery technology [1-3]. They are widely used in varieties of electronic devices due to their good cycle life, high energy density and high capacity over any battery technology. The Li-ion battery technology that now dominates much of the portable battery business has matured enough over the last five years to be considered for the short-term implementation in Hybrid Electric Vehicles (HEV) and Electric Vehicles (EV) applications [1]. However, high cost, safety hazards, and chemical instability of cathode materials have been major concern in the battery industries, which prohibits wider application in the automotive industry [4]. In addition, the volatility of the Li-ion battery technology, has made a massive product recall from the battery industries in recent years. Therefore, increased public awareness about these battery issues solemnly demanding for Li ion batteries with reliability and safety materials.

Among the battery components, the cathode materials are the one which are crucial in determining the high power, safety, longer life and cost of the battery that satisfy the requirement of the larger battery system that can be applicable to electric vehicles, power tools, energy storage equipment and so on [5, 6]. In this context, the olivine-type materials based on lithium transition metal phosphates ($LiMPO_4$ with M=Fe, Mn, Co, Ni) has been emerging as a potential cathode candidate for high power batteries [7]. When compared to the well known layered structure (e.g. $LiCoO_2$) and spinel structure (e.g. $LiMn_2O_4$) based cathode materials, the olivine structured $LiMPO_4$ cathode materials exhibit a flat voltage profile at 3.45-5.1 V vs Li+/Li. Among these, the $LiFePO_4$ and $LiMnPO_4$ cathodes shows the theoretical discharge capacity of about 170 mAhg^{-1}, which make this material a safe cathode material with good cycle life and high power density [5, 6]. However, $LiMPO_4$ materials are basically insulating in nature, hence, has a very poor lithium ionic and electronic conductivity (10^{-9} to 10^{-12} S cm^{-1}). This is because of separation of MO_6 octahedron by the PO_4 tetrahedra, and the one-dimensional chains formed by the edge-sharing LiO_6 octahedra along the b-axis of the orthorhombic structure. Since the first report by Padhi et al., a lot of

effort has been devoted to optimize the electronic conductivity of the material and successfully solved the problem by adding different conductive additives during or after the synthesis. One way to overcome this difficulty was to add carbon, either by use of carbon additive to synthesize the material or adding the carbon source to the precursors during the synthesis process and convert it to thin carbon coating on the surface of cathode particles by carbonization [7]. Other efforts to improve the electronic conductivity includes the addition of dispersed metal powders, doping with several elements and coating with conductive polymers [8-11].

In addition to above conductive coating development, in recent years the efforts to overcome the inherent deficiency of $LiMPO_4$ materials have been focused on reducing the particle size to nanometer scale [12-15]. Some reports indicate that Li^+ diffusion capability may become a controlling step, when the electronic conductivity of the olivine phosphate such as $LiFePO_4$ is optimized [4]. The rate capability of the electrode increases with the decrease of particle size due to the short length of the electronic/ionic transportation and the large specific surface available for electrochemical reaction [16-18]. For example, the lithium-ion diffusion coefficient, DLi, in the cathode $LiFePO_4$ was estimated at 10-14 cm^2s^{-1} from electrochemical impedance spectroscopy. Based on this value, a discharge process of one minute requires a lithium-ion diffusion length of below 7.5 nm, i.e., a particle size below 15 nm [19]. Therefore, unlike in bulk $LiMPO_4$ the Li+ diffusion will be very fast and full capacity can be achieved with nano $LiMPO_4$. Tremendous efforts have been made in recent years to reduce the particle size by employing conventional as well as solution-based synthetic method [6-18]. Different process engineering of $LiMPO_4$ electrode materials had been reported in the literature is shown in the Figure 1, with processing conditions such as reaction temperature and time. Increase in the reaction temperature and reaction time makes the process commercial not feasible due to high cost. Most of the high temperature or energy consuming process, including conventional solid state reaction, usually resulted in the large particle size distribution with particle size ranging from 200-1000 nm due to the high temperature and high energy treatments (Figure 1). Among the various synthetic strategies, the solution based route have witnessed great progress in size control and electrochemical performances [20-26]. For example, solvothermal method has been used to synthesize the $LiFePO_4$ nanoparticles and nanoplates by using organic solvents such as tetraethyleneglycol, benzyl alcohol and ethylene glycol [27-28]. This method shows disadvantages in terms of the expensive solvents and high process temperatures. Murugan et al reported microwave-solvothermal synthesis for phospho-olvine nanorods. This is also one of the suitable processes for rapid one-pot synthesis of electrode materials. However, the particle size was in the range of 50-100 nm. Since 2001, the hydrothermal method has been widely used to prepare the size and morphology controlled $LiMPO_4$ materials [20]. This method offered many advantages such as quick, easy to perform, low cost, energy-saving and easily scalable method to prepare the fine $LiMPO_4$ particles. Conversely, this method requires additional heat treatment step in order to improve the cyrstallinity as well as conductive coating.

Recently, we have reported a rapid, one-pot supercritical fluid (SCF) process for the preparation of size, and morphology controlled $LiMPO_4$ nanocrystals [29-30]. The SCFs provides a number of benefits for preparing size and morphology controlled nanocrystals. These days, the SCFs have been widely studied as a new kind of reaction media for nanomaterials synthesis owing to their unique properties such as gas like diffusivity, low
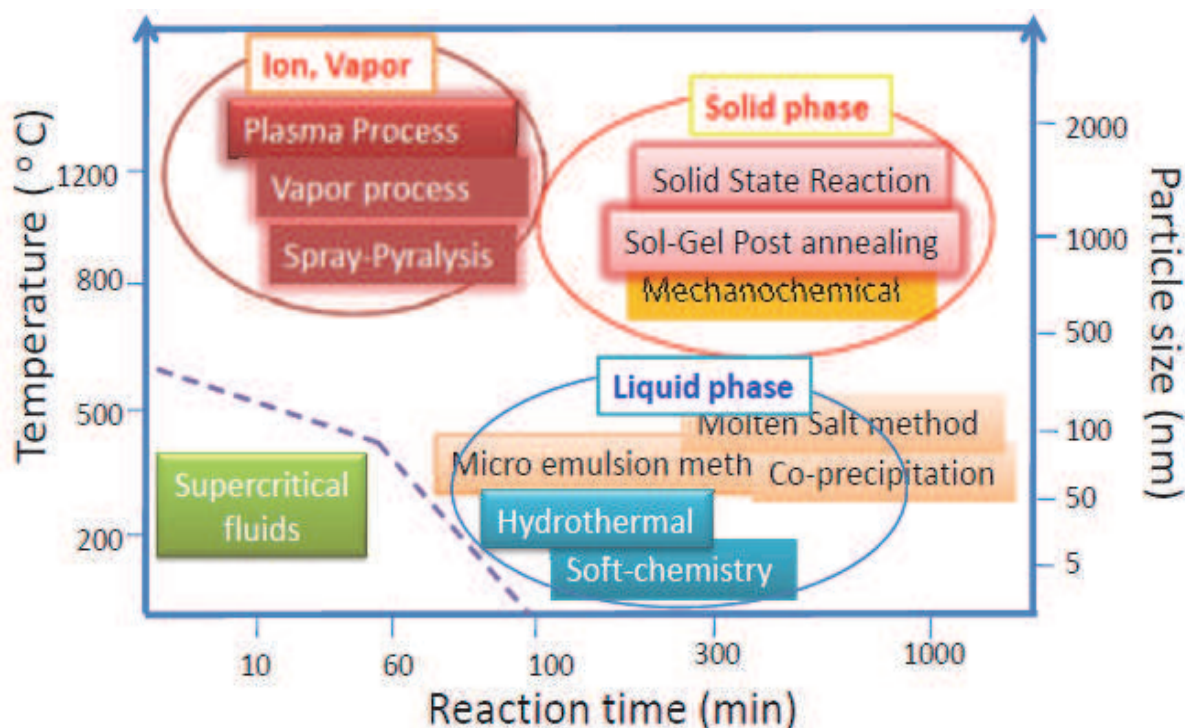
Fig. 1. Process engineering of electrode nanomaterials, the process involving high temperature and high energy species are not feasible for commercialization point of view.

viscosity and the density closer to that of liquid [29-32]. The surface tension completely vanishes above the critical point of the fluid; this is of particular interest in controlling the surface and interface chemistries of the nanostructures. Further, the SCFs forms homogeneous phase with gas or organic compounds. This makes the SCFs a unique reaction medium for the preparation of organic-inorganic hybrid nanostructures.

Progress in the size and morphology control of $LiMPO_4$ nanocrystals have opened up various $LiFePO_4$ nano structures such as irregular nanoparticles, nano rods, nano plates, nanowires and porous nanostructures and so on [33-35]. Organization of such nano scale building blocks into complex hierarchical architectures via self-assembly is of great interest, because of their size and shape dependent physical and chemical properties. However, there are only few reports on the preparation of $LiFePO_4$ hierarchical architectures with well defined size and morphologies.

In this chapter, we present the systematic study of designing $LiFePO_4$ electrode nanocrystals with controlled size, morphology, hierarchical nanostructures and properties by supercritical ethanol (SCE) process. We present the effect of different reaction conditions such as reaction time, temperature, precursor concentration and precursor to the surfactant ratio on the nano structure formation and their surface chemistry. We demonstrate that the supercritical fluid process not only suitable for controlling size, morphology and crystal structures in one pot process, but also facilitates the formation of self assembled hierarchical architectures such as rhombus and dumbbell like structures. We as well demonstrate the decoration of carbon nanotube with $LiFePO_4$ nanocrystals under one-pot supercritical fluid process. The formation mechanism, hierarchical structure, surface chemistry and electrochemical properties of nanostructure electrode will be presented taking $LiFePO_4$ as model nanocrystals electrode material.

2. Experimental section

2.1 Synthesis and self assembly of LiFePO₄ nanostructures

Considering the cost-effective process development, we have used common and cheap solvent ethanol as SCF medium. All the starting material and chemicals were purchased from Wako, chemicals. Firstly, precursor solution was prepared by dissolving $FeCl_2$.$4H_2O$ (0.4 mmol) in 20 ml oleylamine (20-30 mmol) and 16 ml ethanol at a constant temperature of 60 °C for one hour. Solutions of o-H_3PO_4 (0.4 mmol) and Li acetyl acetonate (0.4 mmol) were prepared by dissolving each compound separately in 2 ml of ethanol. These solutions were slowly added to the above mixture under constant stirring. In a typical synthesis $LiFePO_4$ nanostructures, about 5 ml of precursor solution was charged into 10 cc^3 volume stainless steel reactor and heated up to 300-400 °C temperatures and 38 MPa pressure for 4-20 min. Then, the reaction was terminated by quenching the reactor with cold water bath. The resultant $LiFePO_4$ nanostructures were collected by repeated washing and centrifugation with ethanol, followed by drying in a vacuum dry oven at 120 °C for 12 hours. In order to prepare conductive $LiFePO_4$/C, the required amount of as prepared $LiMPO_4$ nanocrystals were dispersed in ethanol. To this 5 weight percent of acetylene black and 10 weight percent of conductive commercial carbon nanotube called VGCF was added as a carbon source under constant magnetic stirring for 6 hours. Later, solution was dried off by evaporating the ethanol at 60 °C. The dried powder sample was collected and subjected to heat treatment at 600 °C for 4 hours under Ar and H_2 gas atmosphere.

Similarly, we prepared the $LiFePO_4$ decorated multi wall carbon nano tube (MCNT) using above precursor but, in the absence of oleylamine. The starting precursor solution was mixed with suitable MCNT (20 weight % of the $LiFePO_4$) and mixed well under magnetic stirrer for 1 hour. Then, the solution was treated 400 °C under SCE conditions and product was obtained as described in the above paragraph.

2.2 Materials characterization

The crystal structure was examined by X-ray diffraction (XRD) analysis with a Bruker AXS D8 Advance instrument using Cu Kα radiation. The morphology was observed by high-resolution transmission electron microscopy (HRTEM; JEOL JEM-2010F). Infrared (IR) spectra of the as prepared materials that were recorded by an FT/IR-6200 IR spectrophotometer (JASCO Corp., Tokyo, Japan).

2.3 Electrochemical cell preparation and characterization

The electrochemical properties of $LiFePO_4$/C nanostructure were studied by assembling a beaker type three electrode cell. The samples were dried overnight at 100 °C in a vacuum before assembling the cell. The dried $LiFePO_4$/C sample was mixed and ground with acetylene black and Teflon (poly(tetrafluoroethylene)) binder in the weight ratio of 90:5:5. The prepared paste was spread uniformly on a 0.1 cm^2 stainless steel SUS sheet (100 mesh) by manually pressing on to the substrate. The cathode loading was 4-5 mg/cm2. Li metal on stainless steel SUS mesh was used as a counter and reference electrodes. The electrolyte consists of the solution of 1 M $LiClO_4$ in ethylene carbonate (EC)/diethyl carbonate (DEC) (1/1 by volume). The cell assembly was carried out in a glove box filled with high purity argon gas. The charge-discharge tests were performed with a Solartron Instrument Model 1287 controlled by a computer in the potential range of 2.0–4.5V versus Li under different current densities.

3. Results and discussion

3.1 Crystal structural analysis LiFePO₄ nanostructures

The powder X-ray diffraction analysis was carried out to confirm the crystal structure and $LiFePO_4$ formation. The crystal structure of the triphylite $LiFePO_4$ has been well studied and documented in the literature [7-15]. The pure $LiFePO_4$ belongs to the olivine of lithium ortho-phosphates with an orthorhombic lattice structure in the space group Pnmb. The structure consists of corner-shared FeO_6 octahedra and edge-shared LiO_6 octahedra running parallel to the b-axis, which are linked together by the PO_4 tetrahedra [36-38]. In our previous study, we have reported the preparation of size, and morphology controlled $LiMPO_4$ nanocrystals by using oleylamine as both reducing as well as capping agent [29]. In this study, we further developed the reaction conditions and obtained $LiFePO_4$ hierarchical structure, by optimizing the oleylamine concentration and reaction time.

Figure 2 shows the XRD patterns of the $LiFePO_4$ nanostructure prepared at 400 ᵒC temperature, for 10 and 20 minute reaction time under supercritical ethanol conditions. All the peaks in the XRD pattern were indexed to an orthorhombic structure with Pnmb space group (JCPDS 40-1499). The peak intensity of the $LiFePO_4$ hierarchical nanostructure formed
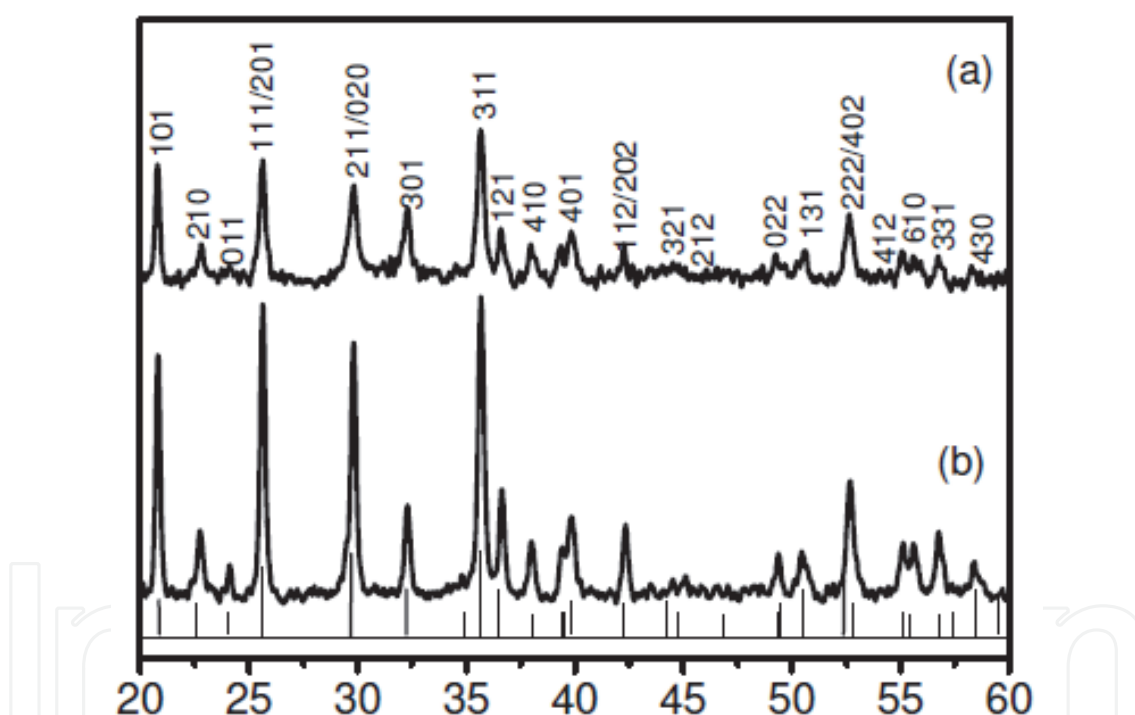

Fig. 2. XRD patterns of the $LiFePO_4$, (a) nano-rods obtained by 8 min reaction; and (b) hierarchical nanostructure obtained by 20 min reaction time at 400 ᵒC.

at 15-20 minutes reaction time is higher than the $LiFePO_4$ nanocrystals formed at 8-minute reaction time as shown in the Figure 2 a and b. This difference in the peak intensity can be attributed to the growth of the $LiFePO_4$ nanstructures with increased reaction time. Effect of reaction time on the hierarchical nanostructural formation is discussed in later section. The XRD patterns clearly show formation of single phase $LiFePO_4$ under supercritical ethanol conditions. The Figure 3 shows the XRD patterns of $LiFePO_4$ nanocrystals prepared at different reaction temperature. The olivine structure $LiFePO_4$ nanocrystals with good crystallinity were obtained at 250 °C temperature. Generally, a high reaction temperature (>

700 °C) or postheat treatment are necessary to prepare the pure and crystalline $LiFePO_4$ particles [13, 20]. It is well known that the $LiFePO_4$ particles prepared by the solution processes without heat treatment possess amorphous $LiFePO_4$ or impurities such as Li_3PO_4 or $Fe_2(PO_4)OH$ or α-Fe_2O_3 along with the $LiFePO_4$ [39]. However, recent progress in solution based techniques demonstrated that using the suitable solution process it is possible to obtain crystalline $LiFePO_4$ nanocrystals around 300-400 °C. By employing SCF process for nanocrystals electrode preparation, the crystalline $LiFePO_4$ nanocrystals were obtained at 250 °C temperature in 10 min reaction time without any post-heat treatment. This is one of the lowest possible temperature reported to obtain the crystalline single phase $LiFePO_4$ nanocrystals. As we can see in the Figure 3, the increased reaction temperature (250-400 °C) had the significant influence on the crystal phase and crystallinity of the prepared samples. The nanocrystals synthesized below 250 °C were not crystalline and included some intermediate phases such as Li_3PO_4. However, as the reaction temperature was increased above 250 °C, the crystallinity was improved and the impurity phases disappeared showing only olivine $LiFePO_4$. Therefore, by taking the advantage of SCE conditions, we could obtain the single phase $LiFePO_4$ nanocrystals at the lowest temperature of 250 °C. The reaction temperature and time played an important role in the formation of well crystalline $LiFePO_4$ nanoparticles under SCE conditions. Because, the temperature above critical point favors the crystallinity of particles, when compared to the subcritical temperature. In addition, the growth of the nanocrystals was controlled by controlling the reaction time between 10-20 minutes. This also had influenced by the rapid heating and homogeneous reaction atmosphere achieved during the SCE process.
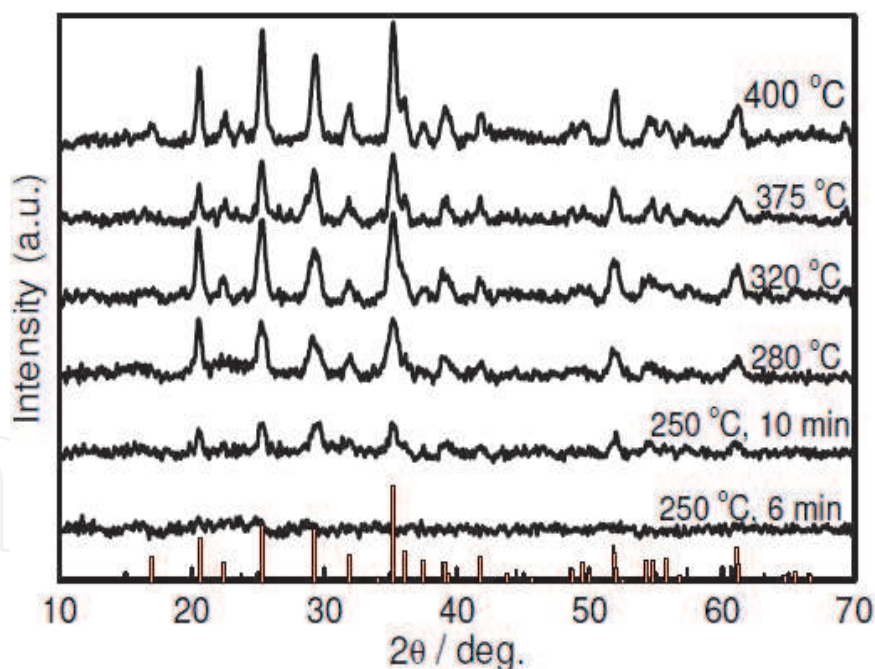

Fig. 3. XRD patterns of the $LiFePO_4$ nanostructure prepared under different reaction temperature and 10 minutes reaction time.

3.2 Surface chemistry of $LiFePO_4$

The surface nature of the $LiFePO_4$ nanostructure has been studied using FTIR spectroscopy and X-ray photoelectron spectroscopy analysis. FTIR spectra provides the information on the organic modification of $LiFePO_4$ nanocrystal surface, which is important in

understanding the formation of self assembled hierarchical nanostructure of $LiFePO_4$. The XPS spectra provide information about the valence state of iron in the nanostructure. This is the direct evidence to understand the effect of oleylamine as reducing agent in controlling the oxidation of Fe^{2+} to Fe^{3+}.

3.2.1 FTIR vibrational spectra

The FTIR absorption spectra of $LiFePO_4$ is shown in Figure 4. There are two classes of vibrational modes reported for $LiFePO_4$ [40]. Internal mode, originate in the intra-molecular
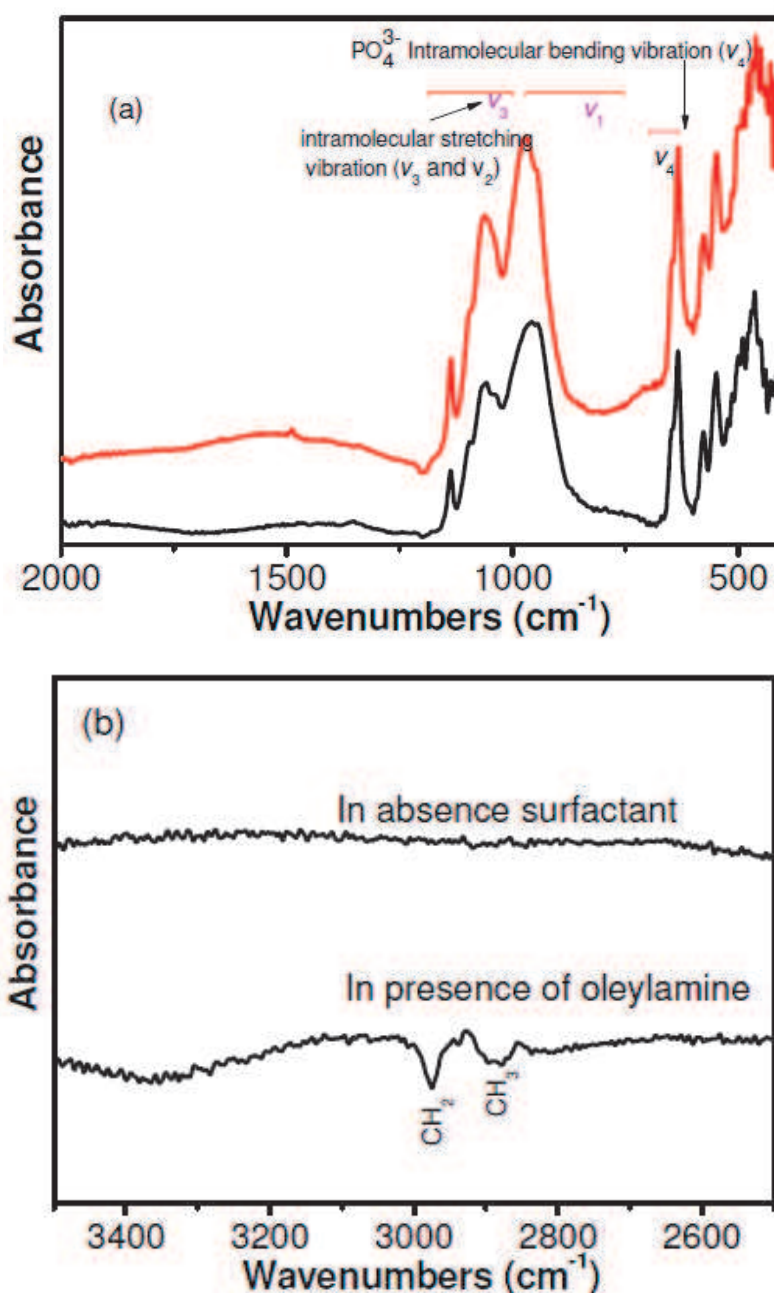
Fig. 4. FTIR spectra of the $LiFePO_4$ nanostructure prepared (a) without oleylamine (top spectrum) and with oleylamine (bottom spectrum) as the surfactant; (b) shows the absence and presence of the C-H stretching mode of methyl and methylene groups, respectively.

vibrations of PO_4^{3-} anion. The vibration of each PO_4^{3-} anion is correlated to those of the other PO_4^{3-} ions in the unit cell, producing a rich vibrational multiplet structure. The bands observed at 943 cm^{-1} and 1042 cm^{-1}, 1068 cm^{-1} and 1140 cm^{-1} are attributed to the intra-molecular stretching *(V$_1$ and V$_3$)* motions of the phosphate anions, respectively. The bands in the region of 643-633 cm^{-1} can be assigned to the bending modes *(V$_4$)* of phosphate anions. The bands in the region of 500-665 cm^{-1} can be assigned to the lithium ion motion. In addition to the confirmation of phosphate anion, we can also study the surface chemistry of nanocrystals using FTIR spectra, especially, when nanocrystals are prepared by surfactant assited synthesis strategy. The Figure 4b shows evidence of capping the LiFePO$_4$ nanocrystals surface with oleylamine ligand molecules by covalent bond formation. As we can see in the FTIR spectra, the organic modified LiFePO$_4$ shows bands in the region 2800-2960 cm^{-1} which are attributed to the C-H stretching mode of methyl and methylene groups. This confirms that LiFePO$_4$ nanostructure surface was coated with organic ligand, which plays a key role in self assembly and hierarchical nanostructure formation of LiFePO$_4$.

3.2.2 XPS spectra of LiFePO$_4$ nanostructure

XPS spectra of LiFePO$_4$ sample is shown in Figure 5. This data confirms the presence of the Fe as Fe^{2+} in LiFePO$_4$. The components of the Fe 2p doublet (Fe 2p$_{3/2}$ and Fe 2p$_{1/2}$), because of spin-orbit splitting, are observed at 712.6 and 726.3eV, respectively, with an energy separation (¢EFe) of 13.5 eV (Figure 5a). The data are in excellent agreement with values of Fe^{2+} reported in the literature [41-42]. These results confirm, within the limit of detection, that no significant oxidation of Fe^{2+} to Fe^{3+} on the surface of the nanostructures occurred during the reaction and the subsequent purification. This shows the importance of oleylamine as reducing as well as capping agent in order to keep the divalent Fe^{2+} in the LiFePO$_4$ nanostructure. The Figure 5b indicates the presence of PO_4^{3-} as the P 2p core level with a binding energy of 133.5 eV. This typical value of binding energy represents P bonded to O [41-44]. By comparing the reported binding energy values of different compounds (132.2-132.9 eV), the P 2p core level at 133.5 eV in this work is attributed to P^{5+} state resulting from the PO_4^{3-} group. Our XPS data are in consistent with what is expected for LiFePO$_4$ on the basis of the structure and chemistry.

3.4 Size and morphology

The influence of oleylamine concentration on the formation of smaller LiMPO$_4$ nanocrystals has been reported in our previous report [29]. We could control the particle size and morphology by controlling the oleylamine and ethanol ratio in the starting precursor solution. For example, LiFePO$_4$ nanocrystals less than 20 nm and 15 nm were obtained, when the oleylamine to the ethanol volume ratio was 20:20 and 20:10 respectively. In the present study, we further extended this work and optimized the oleylamine ratio and reaction time to obtain the self assembled hierarchical nanostructure of LiFePO$_4$. Figure 6 shows the transmission electron microscopy images of the LiFePO$_4$ nanostructure formed under different reaction time and increased amount of oleylamine. When the concentration of oleylamine was increased above 20 mmol, the nano-rods (10-20 nm width) formation was achieved by adjusting reaction time to 8 min at temperature 400 ºC (Figure 6a). These nano-rods started to self assemble by oriented attachment as the reaction time was increased to 10 minutes (Figure 6b). A further increase in the reaction time to 15-20 minutes led to the formation of hierarchical nanostructures via self assembly and shows the different morphology such as dumbbell and rhombus shape, as seen in Figure 8b-f.
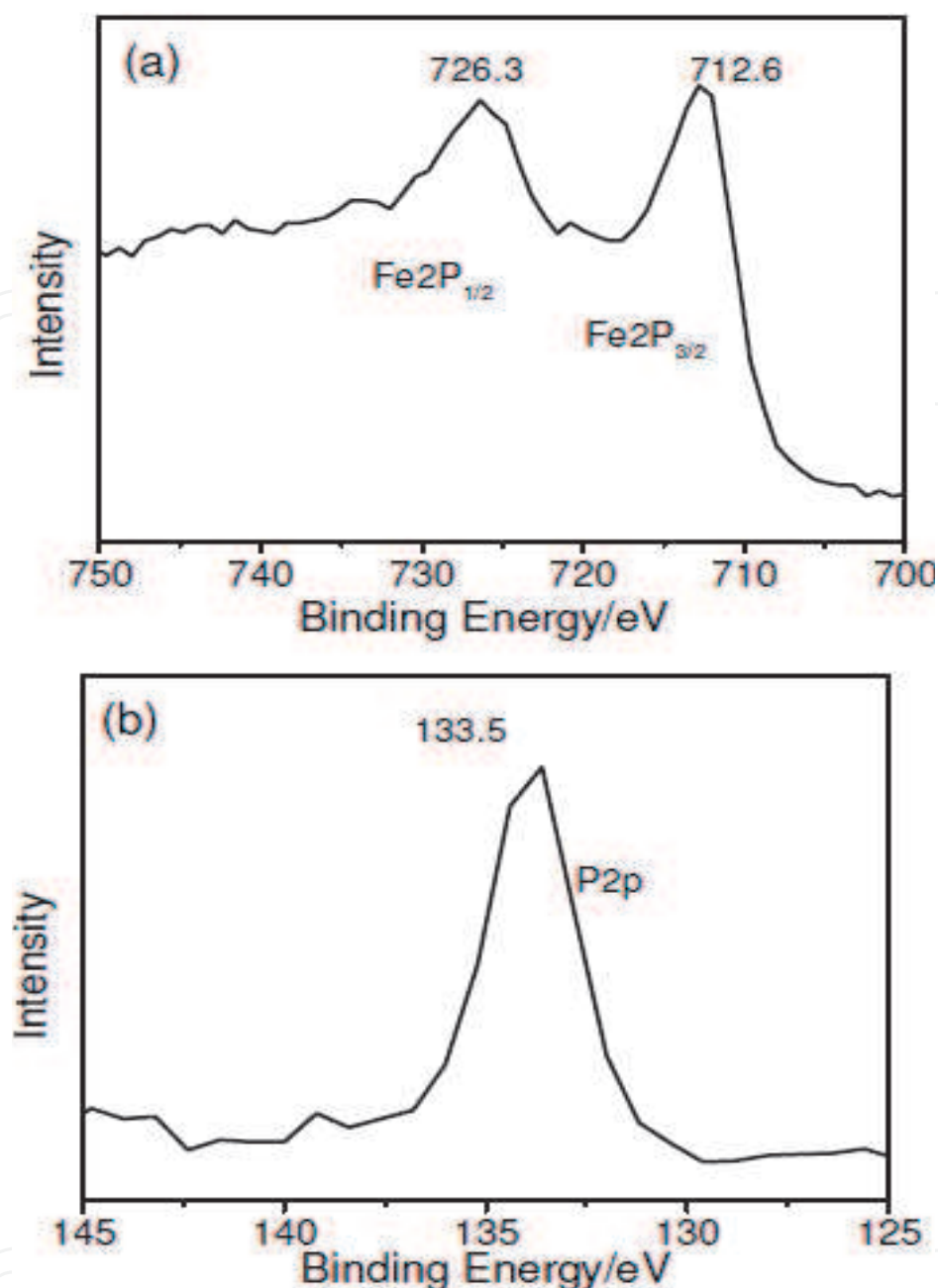
Fig. 5. XPS spectra of the Fe 2p and P 2p core level of the LiFePO$_4$ hierarchical nanostructure synthesized by SCE method.

3.5 Formation of hierarchical nanostructure of LiFePO$_4$

The formation of LiFePO$_4$ hierarchical nanostructure and their formation mechanism was studied in detail by carrying out the time dependent experiments under SCE conditions. The samples were prepared at the different reaction time such as 8 min, 10 min, 15 min and 20 min at 400°C, keeping all the other parameters same. Figure 7 shows the schematic illustrations of formation mechannism and growth of the LiFePO$_4$ nano-rods followed rhombus and dumbbell shape hierarchical nanostructure by the nano rods self assembly. We already had confirmed the formation of the sphere like LiFePO$_4$ nanoparticles with in the 4 min reaction time at 400 ^{o}C temperature in our previous study [29]. Now, by increasing
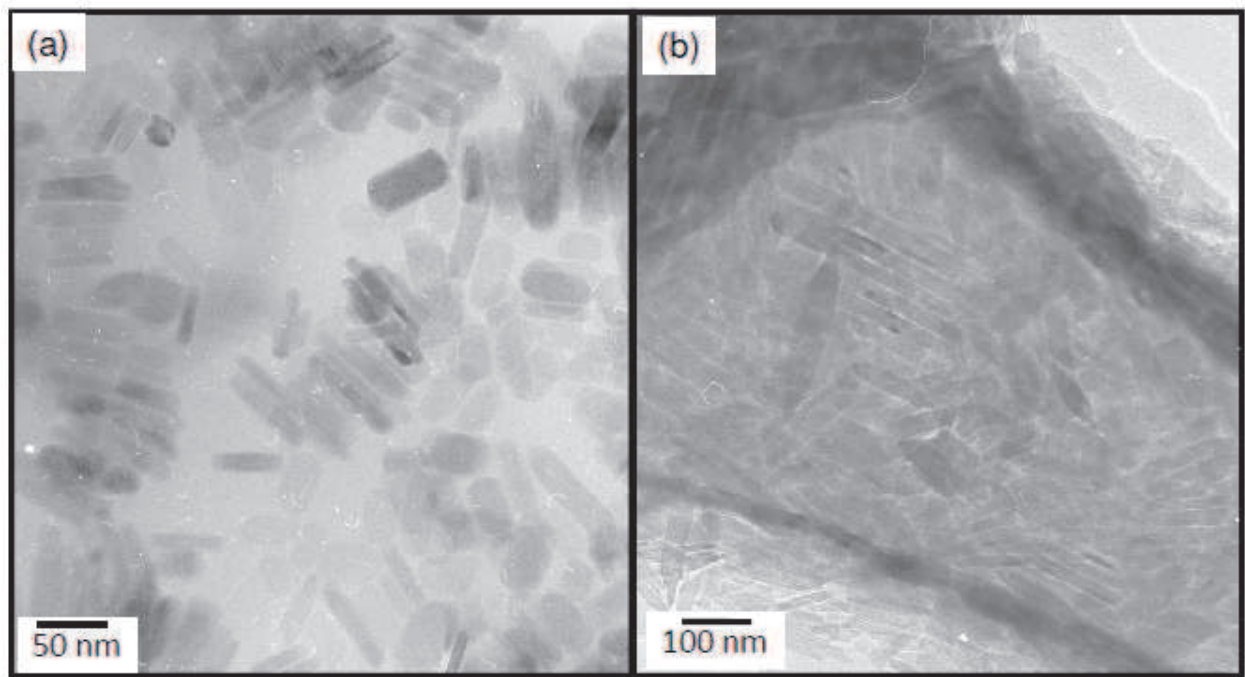
Fig. 6. TEM images of nano rods formed at 8 min reaction time (a), and oriented attachments of nano-rods at 10 minutes reaction time and 400 °C temperature under SCE process.

the reaction time up to 8 min, the nanoparticles continued to grow via elongation into 1D rod like structure as shown in Figure 8a. There are two types rods coexisting at this crystal formation stage, namely, small short nano rods and long rods like structure. As reaction proceeds to 10 minutes, these nanorods aligned by oriented attachement. Figure 8b shows the 4-5 nanorods are aligned by oriented attachment. Finally, further increase with reaction time 15-20 minutes leads to the formation of selfassembled hierarchical nanostructures as shown in Figure 8c-f. We observed the formation of rhombus shape nanostructure at 15 min and with a further increase in the reaction time about 20 minutes led to the dumbbell shape nanostructures formation. The formation of hierarchical nanostructure by self assembly and oriented attachment growth mechanism was also observed by different researchers [45-46]. We have reported formation of $LiFePO_4$ flower like hierarchical microstructure by
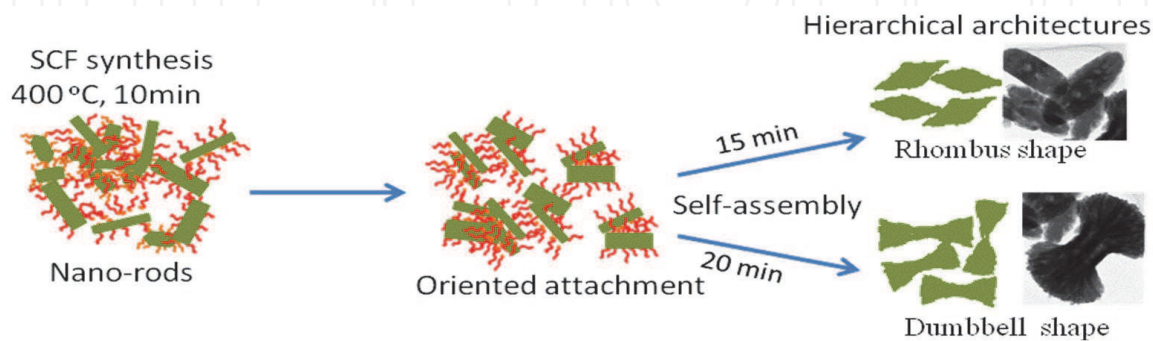

Fig. 7. Schematic illustrations of formation mechannism and growth of the $LiFePO_4$ nanorods and rhombus and dumbbell shape hierarchical nanostructure by nano rods self assembly.

solvothermal reaction using ethylene glycol and hexane as mixed solvent [46]. Zhou et al have successfully prepared highly hierarchical plate like $FeWO_4$ micro-crystals by a simple solvothermal route using ethylene glycol as a capping agent [45]. It was suggested that solvent or surfactant such as ethylene glycol or oleyleamine plays an important role in directing the growth and self-assembly of such unique structures along certain growth direction. It seems that similar reaction mechanism occurs in the present study where oleylamine acts as a soft template in directing the growth of nanoparticles to nano-rods at the early stages through forming hydrogen bonds, and these nano rods further aligned by orientation to form dumbbell and rhombus shape hierarchical structure when the reaction time was prolonged to 15-20 min in the presence of high concentration of oleylamine. As it is well known, oleylamine acts as a surfactant and capping agent, which may greatly affect the size, morphology and microstructure of the products. Thus, the oleylamine molecules may adsorb onto the surface of these nano-rods. It is the interaction of these adsorbed oleylamine molecules that led to the decrease in the rods length and finally formation of hierarchical nanostructure with prolonged reaction time.

3.7 Electrochemical property of LiFePO₄

The electrochemical performance of the $LiFePO_4$ hierarchical nanostructures were studied by charge-discharge measurement. Before the electrochemical measurements, the $LiFePO_4$ sample was heated up to 600 °C in Ar and H_2 atmosphere for 4 hours. As we know from FTIR spectra, the surfactant remains more or less on the surface of the final product, even after being washed several times with ethanol. Considering this, the product was annealed to remove the left surfactant from the surface. In addition, annealing can transform the surfactant into carbon to enhance the electronic conductivity. Therefore, oleylamine not only act as a surfactant to control the size and morphology, but also as a carbon source. Figure 9 displays the charge and discharge curves of the sample at the current density of 0.1 C in the potential range from 2-4.5V. The $LiFePO_4$ hierarchical nanostructure showed a flat discharge voltage at approximately 3.4 V, which represents the typical electrochemical action of Li^+ insertion into $FePO_4$. The charge discharge plateaus of $LiFePO_4$ hierarchical nanostructures is shorter than the $LiFePO_4$ bulk spherical particles that is reported in the literature [21]. The $LiFePO_4$ charge discharge plateau represents the two phase region, where the $FePO_4$ and $LiFePO_4$ coexist during the Li insertion. There are different explanations about the slope of charge-discharge capacity curves. One is the formation of solid solution of Li_xFePO_4 below the certain critical size, for example 40 nm [47]. The second explanation is that pseudo-capacitive effect, which means the charge storage of Li ions from faradaic processes occurring at the surface of the materials. The $LiFePO_4$ hierarchical flower like microstructures formed by the self-assembly of 200-400 nm nano-rods under solvothermal reaction showed the pseudo-capacitive behavior [46]. The pseudo-capacitive effect has been observed for other $LiFePO_4$ hierarchical microstructures such as the dumbbell like structure [48]. However, in the present study, the sample shows very small slope region when compared to those results. The capacity of hierarchical nanostructure offer capacity as high as 154 mAh/g at 0.1-0.5 C with good power capability. This material retains about 70% capacity at 2C with a very good cyclic ability and no noticeable fade as seen in Figure 9b. Therefore, the electrochemical performance of the $LiFePO_4$ hierarchical nanostructure shows promising results that were observed for the $LiFePO_4$ hierarchical microstructures prepared by different synthetic routes.
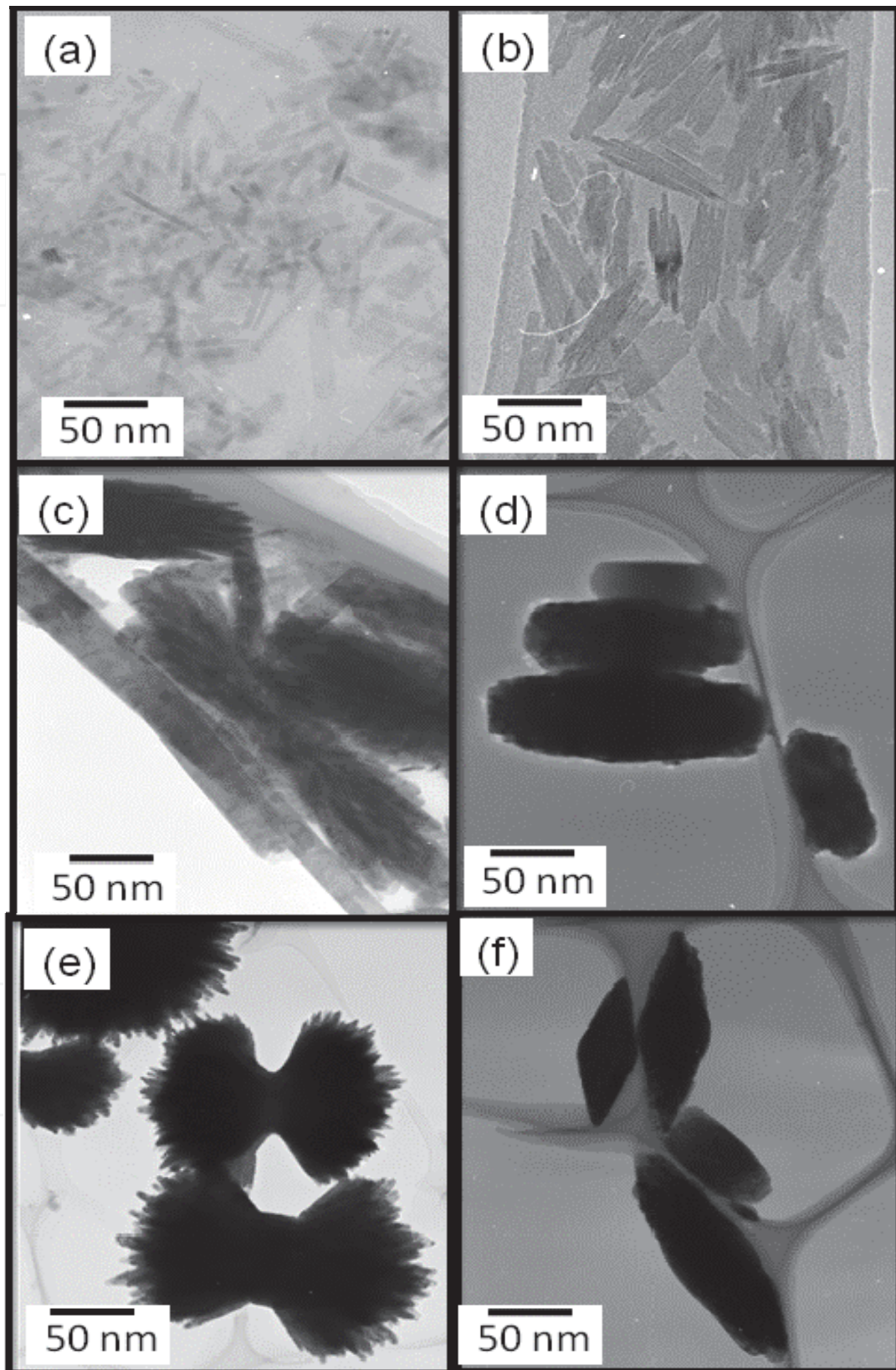
Fig. 8. TEM images of (a) nanorods, (b-c) aligned nanorods, (d, f) rhombus, and (e) dumbbell like hierarchical microstructures of the LiFePO$_4$ obtained at the different reaction time.
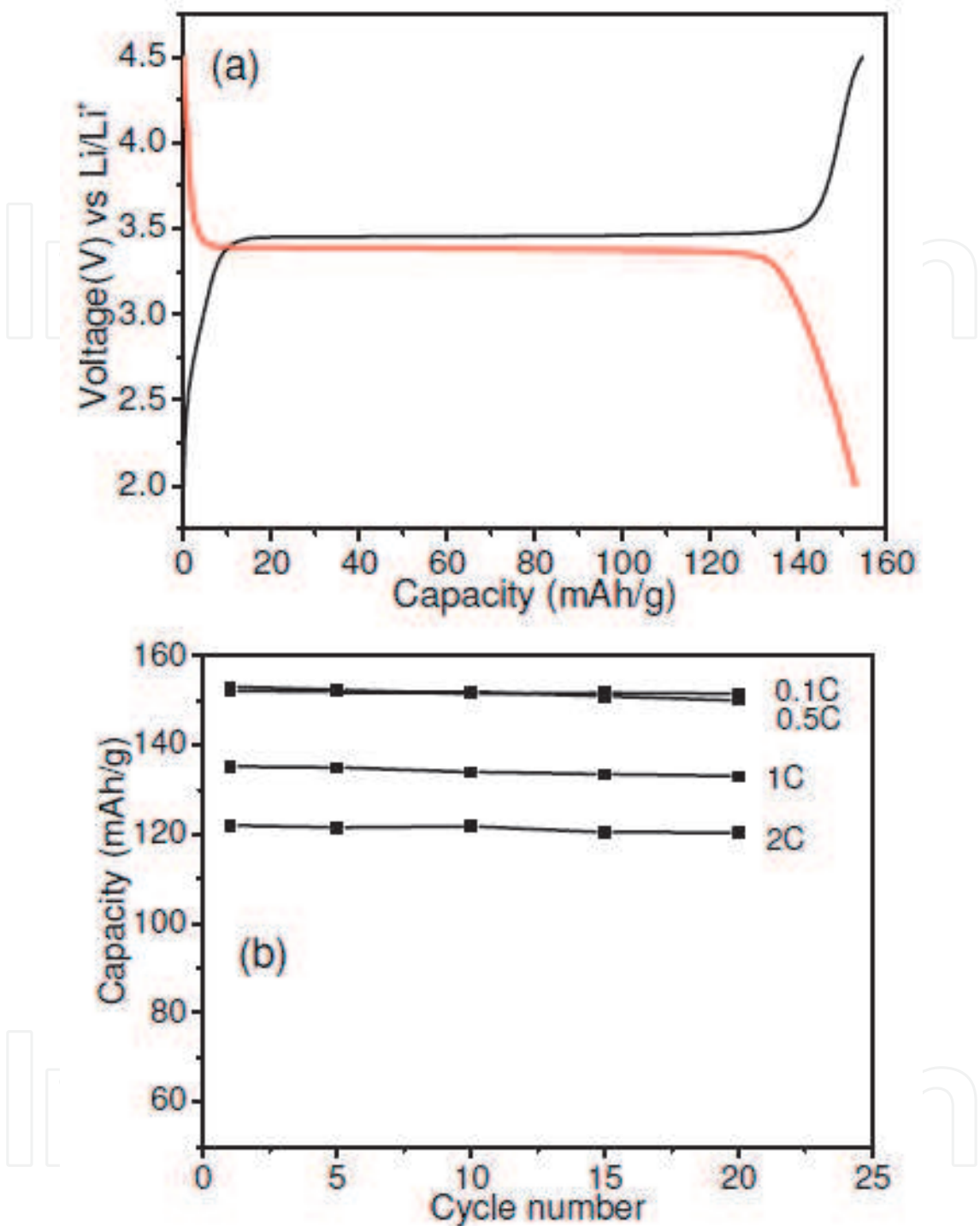
Fig. 9. Charge-discharge profile of the $LiFePO_4$ hierarchical nanostructure measured at 0.1 C (a), along with the rate capability and cyclic performance (b).

3.6 The decoration of carbon nanotube with LiFePO₄ nanocrystals

Preparation of carbon nano-tube and electrode materials hybrid nanostructure is very helpful in improving the electro activity of electrode materials such as Si, Sn, TiO_2 and so on, especially in improving the cycle life and discharge/charge rate capability of electrode materials [49-52]. Designing the $LiFePO_4$ electrode nanostructure with conductive carbon

shows the improved performance of cathode material. Furthermore, addition of conductive metal oxide to olivine nanostructure cathode material can create the electronic conducting networks. The combination of both the nano size and conducting network is effective as the diffusion length for both electrons and ions is reduced to only several nanometers. Recently, the synthesis of C-LiFePO$_4$:RuO$_2$ nano-composite was reported and this composite showed a high rate capability when used as cathode materials for lithium ion batteries [53]. However, the RuO$_2$ is an expensive material; a cost-effective alternate is desired for such nanostructure. Carbon is one of the best choices because of its high electronic conductivity, good lithium permeation, and electrochemical stability. The carbon-coating technique is widely applied for olivine cathode materials. However, the synthesis of such nano composite is complicated and the thickness of carbon shell needs to be controlled to a few nanometers and high temperature in such process is involved.

In recent years, the SCF has been the most popular choice of the reaction media for the preparation of single metal/metal oxide decorated carbon nano-tube composites [50, 54]. The unique features of SCF such as low viscosity, high diffusivity, near zero surface tension and strong solvent power facilitates the formation of hybrid materials with special structures and functions under SCFs conditions. For example, Wai et al. decorated metal nanoparticles (Pd, Ru, Rh) on CNTs and also fabricated Pd, Ni, and Cu nano-wires and nano-rods from the hydrogen reduction of organo-metallic precursors in supercritical CO$_2$ using CNTs as templates [49-50] for catalytic application. Preparation of Ru metal nanocrystals decorated CNTs under supercritical water condition was reported by Sun et al. [54]. In addition, several other metal oxides decorated CNT were prepared by the decomposition of metal salts under supercritical carbon dioxide and ethanol solution at a low temperatures 100-150°C. However, one-pot preparation of CNT with electrode nanocrystals such as LiFePO$_4$ has not been reported. In this section, we have focused our studies on the decoration of MCNT with the LiFePO$_4$ nanocrystals in one-pot SCE synthesis method.

The LiFePO$_4$ decorated MCNT were synthesized by one-pot reaction of starting precursor solution with commercial MCNT under SCE conditions as shown in the schematic representation in the Figure 10. At first, the starting precursor solution was mixed with suitable MCNT (20 weight % of the LiFePO$_4$) and mixed well under magnetic stirrer for 1 hour. During the mixture, the precursor solution was adsorbed on to the surface of MCNT. The LiFePO$_4$ nanocrystals were deposited on the surface of MCNT when the solution was heated up to 400 $^{\circ}$C temperatures and 38 MPa pressure for 10 min. During the SCE reaction, the precursor solution decomposes and the LiFePO$_4$ nanocrystals were deposited on the surface of the MCNT as shown in the Figure 10.

The LiFePO$_4$ decorated MCNT hybrid composite material produced herein have been characterized by different analytical methods such as X-RD and HRTEM to confirm the formation of LiFePO$_4$ decorated MCNT hybrid structure under supercritical ethanol process. The Figure 11, shows the XRD pattern of the LiFePO$_4$ decorated MCNT hybrid composite material. The XRD pattern indicates the formation of the single phase LiFePO$_4$ on the MCNT support. All the peaks observed can be indexed to the olivine structured LiFePO$_4$ with a *Pnmb space group* (JCPDS 40-1499). The peaks for MCNT was not observed as surface of the MCNT is completely covered with nanocrystals. The particle size of the single nanocrystals calculated from the XRD data using Scherrers equation is about 50 nm. This data is in good agreement with the size observed in the TEM images.
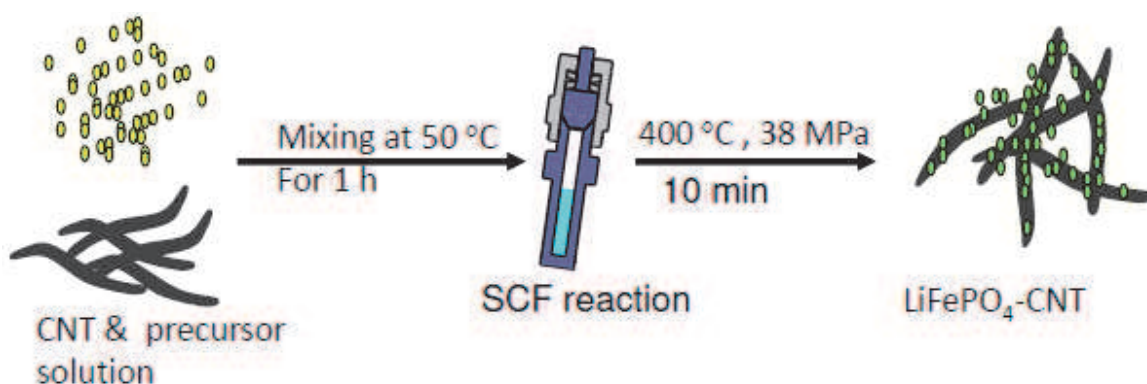
Fig. 10. Schematic illustration of preparation of the LiFePO$_4$ decorated MCNT by using SCE process.
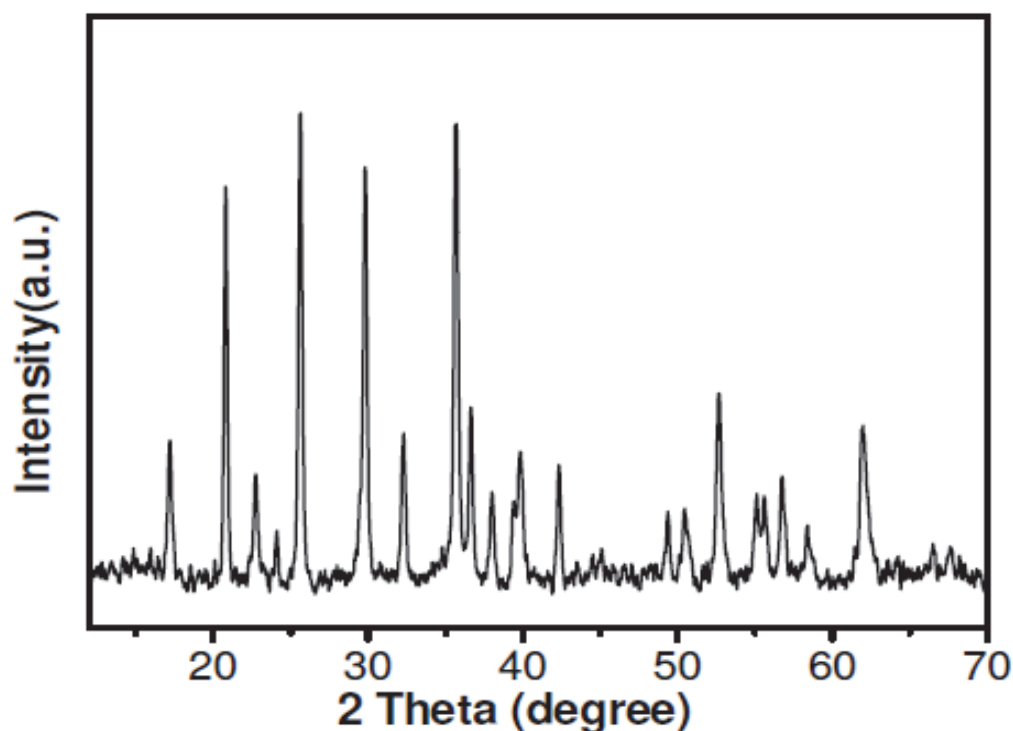

Fig. 11. XRD pattern of the LiFePO$_4$ decorated MCNT nano composite synthesized under SCE conditions at 400 °C for 10 min reaction.

The TEM images of LiFePO$_4$ nanocrystals deposited on the MCNT are shown in Figure 12. The TEM images show that the LiFePO$_4$ nanocrystals are deposited on the surface of MCNT having a plate like morphology with average particle size of 50-100 nm. The size were bigger than the LiFePO$_4$ nanocrystals prepared in the presence of oleylamine without MCNT support as described in the previous section. However, we can further control the particle size by optimizing the reaction conditions and/or using the oleylamine as capping agent and this study is under progress. It was reported that carbon nanotubes surface could be wetted by fluid whose surface tension does not exceed about 200 m N m_1 [50]. It is well known that, the surface tension of the SCF is near zero. Therefore, carbon nanotubes can be wetted during the process to prepare LiFePO$_4$/MCNT composites under SCE conditions. We have confirmed the stability of LiFePO$_4$ nanocrystals coated on the MCNT surface by

repeated washing and prolonged ultrasonic treatment. It was found that the nanoparticles could not be separated from MCNTs even after ultra-sonication treatment; this indicates that attachment of the nanocrystals on MCNTs is very strong.
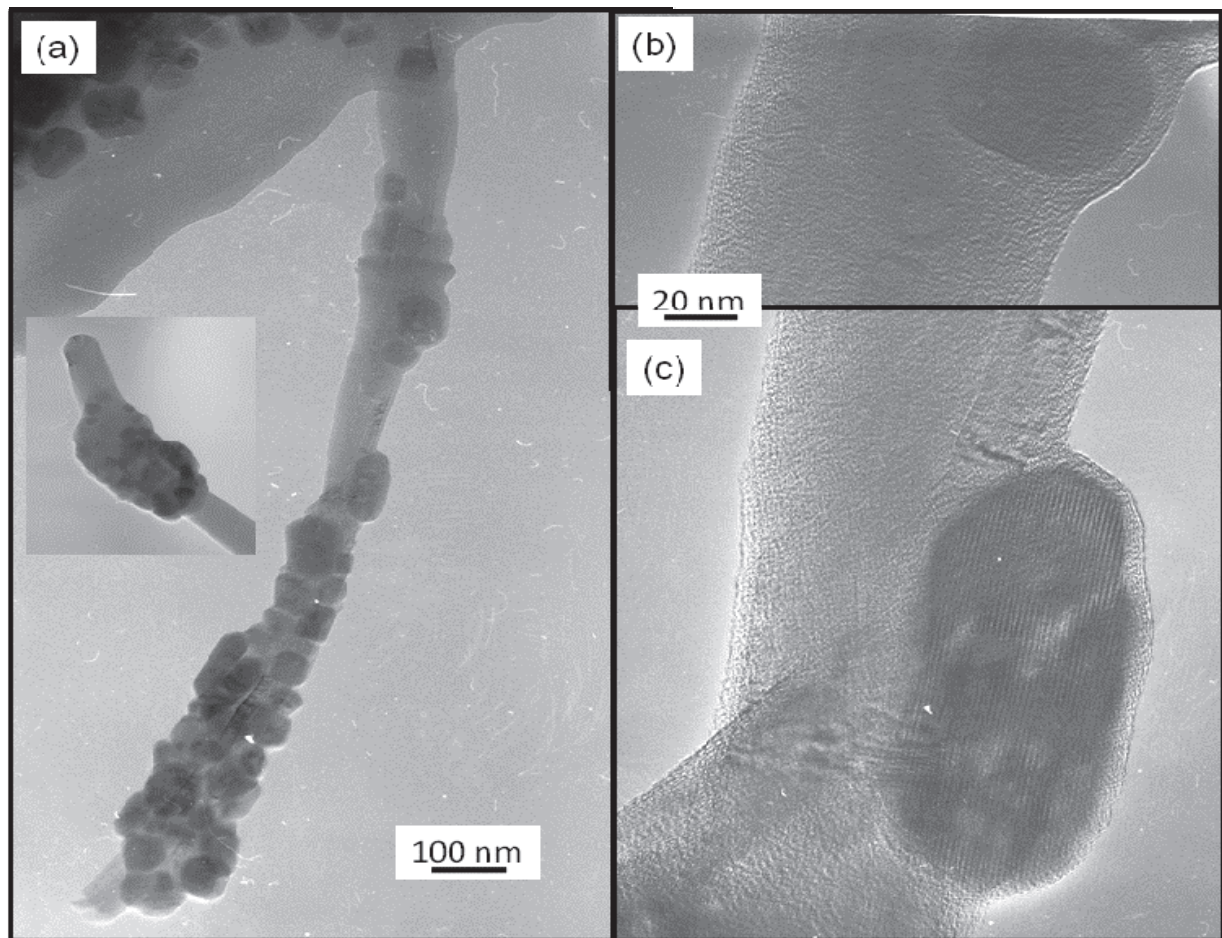

Fig. 12. TEM images of the LiFePO$_4$ nanocrystals deposited on the MCNT (a); and the HRTEM images of the single LiFePO$_4$ nanocrystals deposited on the MCNT (b-c) under SCE conditions at 400 ^{o}C for 10 min reaction.

The electrochemical properties of the LiFePO$_4$ nanocrystals deposited MCNT samples were studied by measuring the charge-discharge performance at 0.1 C. The as prepared sample was just mixed with 10 weight % acetylene black and 5 weight % conductive PEDOT polymer before preparing the electrode. Figure 13 shows the charge-discharge profile of the LiFePO$_4$ nanocrystals deposited on MCNT samples. The initial charge-discharge capacity of about 120 mAh/g at 0.1C rate was observed for this material. This result are interesting considering that the nano composite was prepared in one-pot synthesis by the SCE process at 400 ^{o}C, without any high temperature heat treatment and carbon coating methods. This capacity is comparable to some of the high temperature processed LiFePO$_4$ results [10,11]. The measured specific capacity was about 70 % of theoretical capacity. This sample also showed good cyclic performance with a very little change in capacity after 30 cycles (data is not shown here). Considering the low processing temperature, the LiFePO$_4$ nanocrystals deposited on the MCNT sample shows a promising discharge capacity. A study to optimize

the synthesis conditions and electrochemical performance of this material is under progress and will be reported in near future.
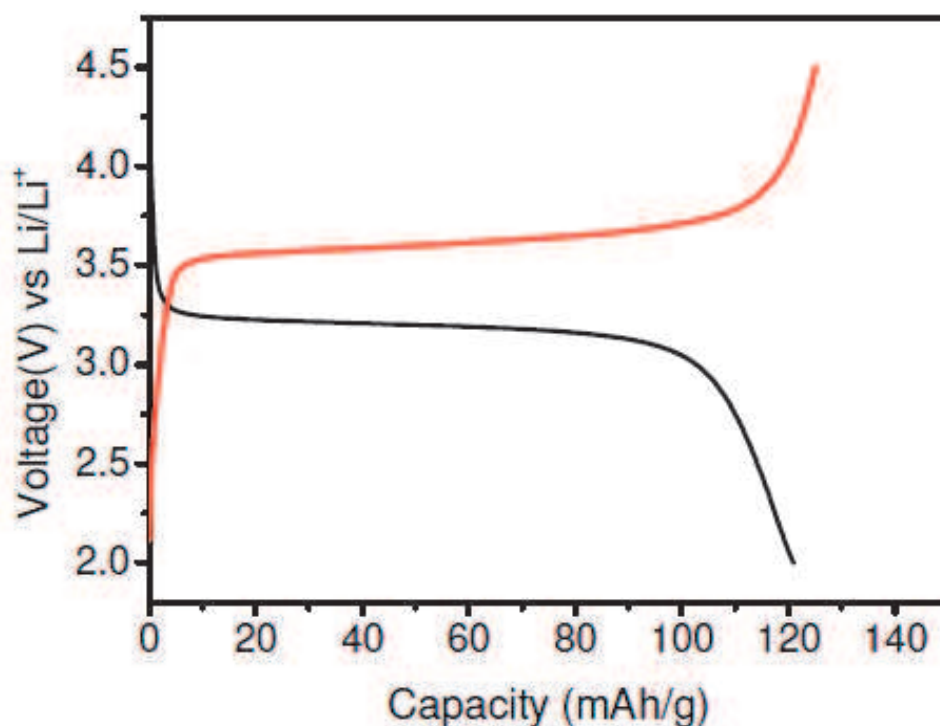

Fig. 13. Charge-discharge profile of the LiFePO$_4$ decorated CNT nano composite measured at 0.1C.

3. Conclusion

In summary, we have successfully demonstrated the designing the LiFePO$_4$ electrode hierarchical nanostructures using SCE process. The self assembly of hierarchical nanostructures such as rhombus and dumbbell like structures were obtained by controlling different reaction conditions such as reaction time and precursor to the surfactant ratio. These parameters had significant effect on the nano structure formation and their surface chemistry. It was observed that the SCE process is not only suitable for the controlling size, morphology and crystal structures in one pot process, but also facilitates the formation of self assembled hierarchical architectures. The formation mechanism studies shows that oriented attachment and growth were responsible for the hierarchical nanostructures formation under supercritical conditions, in the presence of oleylamine as reducing and capping agent. The charge-discharge capacity of hierarchical nanostructure sample was about 154 mAh/g at 0.1-0.5 C, which is about 90 percent of theoretical capacity of the material. This material also showed a good rate capability and retains about 70% capacity at 2C with a very good cyclic stability. The electrochemical performance of the LiFePO$_4$ hierarchical nanostructure shows promising results that were observed for the LiFePO$_4$ hierarchical microstructures prepared by different synthetic routes.

We also demonstrated the decoration of MCNT with LiFePO$_4$ nanocrystals under one-pot SCE process. The formation LiFePO$_4$ decorated MCNT bybrid nanocmposite and their morphology was confirmed by XRD and TEM analysis. About 50-100 nm size nanocrytals

were deposited on the surface of the MCNT was observed. The electrochemical properties of this composite show charge-discharge capacity about 120mAh/g at 0.1C. Further studies should be carried out in order to improve the electrochemical performance of this hybrid structure.

4. Acknowledgment

5. References

[1] Tarascon, J.-M. Armand, M. *Nature,* (2001) 414, 359–367.

[2] Arico, A.S, Bruce, P. Scrosati, B. Tarascon J.M. Schalkwijk W.V. (2005), 4, 366-377.

[3] Nazar, L. F. & Crosnier, O. In *Lithium Batteries Science and Technology* (eds Nazri, G.-A. & Pistoia, G.) 112–143 (Kluwer Academic/Plenum, Boston, 2004).

[4] Tarascon, J.M. Recham, N. Armand, M. Chotard, J.N. Barpanda, P. Walker, W. Dupont, L. Chem. Mater. (2010) 22, 724-739.

[5] Ellis, B.L. Lee, KZ.T. Nazar, L.F. *Chem. Mater.* (2010) 22, 691-714.

[6] Padhi, A.K. Nanjundaswamy, K.S. Goodenough J.B. *J. Electrochem. Soc.* (1997), 144, 1188.

[7] Ravet, N. Goodenough, J. B. Besner, S, Simoneau, M. Hovington, P. Armand, M. Procceings of the 196th ECS Meeting, Honolulu, october 1999.

[8] Huang, H. Yin, S.-C. Nazar, L. F. *Electrochem. Solid State Lett.* (2001) 4, 10, A170.

[9] Yamada, A. Chung, S. C. Hinokuma K. *J. Electrochm. Soc.* (2001) 148, A224.

[10] Wang, Y. Wang, J. Yang, J. Nuli, Y. *Adv. Funct. Mater.* (2006) 16, 2135.

[11] Franger, S. Cras, F. L. Bourbon, C. Rouault, H. *Electrochem. Solid-State Lett.* (2002) *5*, A231.

[12] Yang, S. Zavalij, P. Y. Whittingham, M. S. *Electrochem. Commun.*, (2001) *3*, 505.

[13] Shiraishi, K. Dokko, K. Kanamura, K. *J. Power Sources*, (2005) *146*, 555.

[14] Wang, G. X. Bewlay, S. Needham, S. A. Liu, H. K. Liu, R. S. Drozd, V. A. Lee, J.-F. Chen, J. M. *J. Electrochem. Soc. (*2006), *153*, A25.

[15] Park, K. S. Kang, K. T. Lee, S. B. Kim, G. Y. Park, Y. J. Kim, H. G. *Mater. Res. Bull. (*2004), *39*, 1803.

[16] *Poizot*, *P.* Laruelle, S. Grugeon, S. Dupont, L. Tarascon, J-M. *Nature,* (2000), 407, 496-499.

[17] *D. Larcher*, C. Masquelier, *D.* Bonnin, Y. Charbre, V. Masson,. J.B. Leriche *J. Electrochem. Soc.* (*2003*) *150*, A133.

[18] *Armstrong*, *R.*; *Armstrong*, G.; Canales, J.; Garcia, *R.*; Bruce, P. *Adv. Mater.* (*2005)*, *17, 862.*

[19] Wang, Y. Li, H. He, P. Hosono, E. Zhou, H., Nanoscale, (2010), 2, 1294-1305.

[20] Yang, S. Zavalij, P. Y. Whittingham, M. S. *Electrochem. Commun.*(2001), 3, 505– 508

[21] Xiao, J. Xu, W. Choi, D. Zang, J-G. *J. ElectroChem.Soc. (*2010), 157, A141-A147,

[22] Drezen, T.; Kwon, N.; Bowen, P.; Teerlinck, I.; Isono, M.; Exnar, I. *J. Power Sources* (2007), 174, 949– 953,

[23] Delacourt, C.; Poizot, P.; Morcrette, M.; Tarascon, J.-M.; Masquelier, C. *Chem. Mater.* (2004), 16, 93– 99.

[24] Lim, J.; Kim, D.; Mathew, V.; Kim, J; Phys. Scr. (2010), T139, 014060,

[25] Murugan, A.V. Muraliganath, T. Manthiram, A. *Electrochem. Comm.* (2008), 10, 903

[26] Wang, D. Buqa, H. Crouzet, M. Deghenghi, G. Drezen, T. Exnar, I. Kwon, N-H. Miners, J. H. Poletto, L. Gratzel, M.*J. Power Sources,* (2009), 189, 624.

[27] Kim D. H. and Kim, J. *Electrochem. Solid-State Lett.*, (2006), 9, A439

[28] Murugan, A. V. Muraliganth T. Manthiram, A. *Electrochem. Commun.*, (2008), 10, 903

[29] Rangappa, D.; Sone, K.; Kudo, T.; Honma, I.; *Chem. Commun.* (2010) 46, 7548.

[30] Rangappa, D.; Ichihara, M.; Kudo, T.; Honma, I.; *Journal of Power Sources,* (2009), 194, 1036–1042.

[31] Veriansya, B.; Kim, J-D.; Min, B. K.; Shin, Y. H.; Lee, Y-W.; Kim. J.; *The J. Supercritical Fluids,* (2010), 52, 76-83,

[32] Rangappa, D.; Ohara. S.; Naka, T.; Kondo, A.; Ishii, M.; Adschiri, T. *J. Am.Chem.Soc.* (2007), 129, 36, 11064

[32] Adschiri, T.; Hakuta, Y.; Arai, K.; *Ind. Eng. Chem. Res.* (2000), *39,* 4901.

[33] Ellis, B. Kan, W. H. Makahnouk, W. R. M. Nazar, L. F. *J. Mater. Chem.* (2007), 17, 3248.

[34] Dominko, R. Bele, M. Goupil, J. M. Gaberscek, M. Hanzel, D. Arcon, I. Jamnik, J. *J. Chem. Mater.* (2007), 19, 2960.

[35] Saravanan, K. Reddy, M. V. Balaya, P. Gong, H. Chowdari, B.V. R. Vittal, J. J. *J. Mater. Chem.* (2009), 19, 605.

[36] Franger, S. Cras, F. L. Bourbon, C. Rouault, H. *Electrochem. Solid-State Lett.* (2002), *5,* A231.

[37] Islam, M. S. Driscoll, D. J. Fisher C. A. J. and Slater, P. R. *Chem. Mater.* (2005), 17, 5085.

[38] Zaghib, K. J. B. Goodenough, A. Mauger, Gendron F. Julien, C. M. *Chem. Mater.*, (2007), 19, 3740

[39] Dokko, K. Shiraishi, K. Kanamura, K.*J. Electrochem. Soc.* 152 (2005), 11, A2199.

[40] Christopher, M. B, Roger, F. *Spectrochimica Acta Part A* (2006), *65,* 44.

[41] Herstedt, M.; Stjerndahl, M.; Nyten, A.; Gustafsson, T.; Rensmo, H.; Siegbahn, H.; Ravet, N.; Armand, M.; Thomas, J. O.; Edstrom, K. *Electrochem. Solid-State Lett.* (2003), *6,* A202.

[42] Dedryvere, R. Maccario, M. Croguennec, L. Cras, F.L. Delmas, C. Gonbeau, Chem. Mater. (2008), 20 7, 164-7170.

[43] Briggs, D.; Seah, M. P. *Practical Surface Analysis by Auger and XPS*; Wiley: New York, (1985), p 37.

[44] Morgan, W. E.; Van Wazer, J. R.; Stec, W. J. *J. Am. Chem. Soc.*(1973), *95,* 751.

[45] Zhou, Y.-X. Yao, H.-B. Zhang, Q. Gong, J.-Y. Liu, S.-J. Yu, S.-H. *Inorg. Chem.*, (2009), 48, 1082.

[46] Rangappa, D.; Sone, K.; Kudo, T.; Honma, I.; *Journal of Power Sources,* (2010) 195, 6167–6171.

[47] Gibot, P. Cabanas, M. C. Laffont, L. Levasseur, S. Carlach, P. Hamelet, S. Tarascon, J. M. Masquelier, C. *Nat. Mater.* (2008), 7, 741.

[48] H. Yang, X-L. Wu, M-H. Cao and Y-G. Guo, *J. Phys. Chem. C,* (2009), 113, 8 3345.

[49] Ye XR, Lin YH, Wang CM, Wai CM. Adv Mater (2003) 15, 4, 316

[50] Ye XR, Lin YH, Wang CM, Engelhard MH, Wang Y, Wai CM. J Mater Chem, (2004), 14, 5, 908–13.

[51] Fu, L. Liu, Z. M. Liu, Y. Q. Han, B. X. Wang, J. Q. and Cao, L. C. Adv. Mater. (2004) 16, 350

[52] Sakamoto J.S. Dunn, B. J. Electrochem. Soc. (2002), 149, A26

[53] Hu, Y.-S. Guo, Y.-G. Dominko, R. Gaberscek, M. Jamnik, J. Adv.Mater. (2007), 19, 1963.

[54] Sun ZY, Liu ZM, Han BX, Wang Y, Du JM, Xie ZL, Adv Mater (2005) 17, 7, 928–32
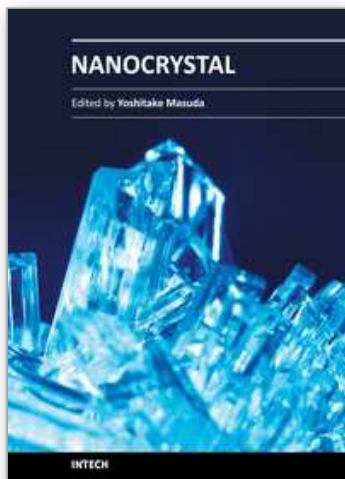
Nanocrystal

Edited by Dr. Yoshitake Masuda

We focused on cutting-edge science and technology of Nanocrystals in this book. "Nanocrystal" is expected to lead to the creation of new materials with revolutionary properties and functions. It will open up fresh possibilities for the solution to the environmental problems and energy problems. We wish that this book contributes to bequeath a beautiful environment and valuable resources to subsequent generations.

How to reference

In order to correctly reference this scholarly work, feel free to copy and paste the following:

Dinesh Rangappa and Itaru Honma (2011). Designing Nanocrystal Electrodes by Supercritical Fluid Process and Their Electrochemical Properties, Nanocrystal, Dr. Yoshitake Masuda (Ed.), ISBN: 978-953-307-199-2, InTech, Available from: http://www.intechopen.com/books/nanocrystal/designing-nanocrystal-electrodes-by-supercritical-fluid-process-and-their-electrochemical-properties

INTECH
open science | open minds